ACS APPLIED MATERIALS & INTERFACES

Research Article

www.acsami.org

# Bioinspired Design of an Immobilization Interface for Highly Stable, Recyclable Nanosized Catalysts

Insu Kim,[†] Ho Yeon Son,[†] Moon Young Yang,[‡] and Yoon Sung Nam*[,†,‡]

[†]Department of Materials Science and Engineering and [‡]KAIST Institute for NanoCentury (KINC CNiT), Korea Advanced Institute of Science and Technology (KAIST), 291 Daehak-ro, Yuseong-gu, Daejeon 305-701, Republic of Korea

Supporting Information

**ABSTRACT:** Immobilization of nanometer-sized metal catalysts into porous substrates can stabilize the catalysts and allow their recycled uses, while immobilization often sacrifices the active surface of catalysts and degenerates the local microenvironments, resulting in the reduction of the catalytic activity. To maintain a high activity of immobilized nanocatalysts, it is critically important to design an interface that minimizes the contact area and favors reaction chemistry. Here we report on the application of mussel-inspired adhesion chemistry to the formation of catalytic metal nanocrystal−polydopamine hybrid materials that exhibit a high catalytic efficiency during recycled uses. Electrospun polymer nanofibers are used as a template for in situ formation and immobilization of gold nanoparticles via polydopamine-induced reduction of ionic precursors. The prepared hybrid nanostructures exhibit a recyclable catalytic activity for the reduction of 4-nitrophenol with a turnover frequency of 3.2−5.1 $\mu$mol $g^{-1}$ $min^{-1}$. Repeated uses of the hybrid nanostructures do not significantly alter their morphology, indicating the excellent structural stability of the hybrid nanostructures. We expect that the polydopamine chemistry combined with the on-surface synthesis of catalytic nanocrystals is a promising route to the immobilization of various colloidal nanosized catalysts on supporting substrates for long-term catalysis without the physical instability problem.

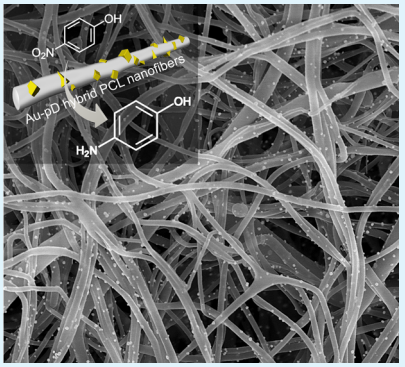


**KEYWORDS:** *catalysis, metal nanoparticles, polydopamine, electrospinning, poly(ε-caprolactone)*

## 1. INTRODUCTION

Nanometer-sized colloidal catalysts have received increasing attention because of unique optical and electronic properties derived from nanoscale-confined structures and a large surface area-to-mass ratio.[1] However, two technical issues restrict their wide applications. First, the separation and recovery of such catalytic nanoparticles in their isolated form is very challenging due to their small sizes.[2] Residual nanocatalysts are generally considered very undesirable because of their potential harmful impact on ecosystems.[3] The other issue is related to the dispersion and structural instability of nanoparticles, which can greatly reduce their catalytic activity, making the nanocatalysts inappropriate for long-term applications.[4−6]

To overcome such limitations, various immobilization approaches have been attempted using porous supporting substrates.[2,5,7,8] Widely used supporting materials include silica structures (e.g., gels, beads, sand, and fiber meshes),[9] zeolites,[10] microporous cellulose membranes,[11] and alumina silicate microspheres.[12] The strong binding of catalysts to the supporting substrate is an essential requirement for long-term uses of catalyst; however, it was reported that the increased adhesion strength of catalysts to the substrate can ironically reduce the intrinsic catalytic activity because of reduced active surface area. Limited mass transfer, light scattering, and toxificiation of catalysts were also observed in immobilized catalytic systems. Therefore, it is very important to develop a technique that can guarantee the high specific catalytic activity of nanocatalysts while maintaining their long-term structural stability.

Three-dimensional porous supporting substrates can be fabricated by a variety of techniques, including porogen leaching, phase separation, gas foaming, colloidal templating, and electrospinning.[13−18] Among these techniques, recent studies highlighted the use of electrospun nanofibers because of the applicability to various polymeric and composite materials, facile optimization of the pore size, porosity, and mechanical properties, and relatively cheap and feasible scale-up production. The surface functionalization of electronspun nanofibers with catalytic inorganic nanoparticles has been performed through photoinitiated, thermal, or chemical reduction of inorganic precursor ions, and layer-by-layer deposition.[5,19]

Recently, mussel-inspired surface modification was developed as a facile method for coatings of various organic and inorganic substrates via the oxidative polymerization of dopamines into polydopamine (denoted "pD").[20] pD coatings can generate a highly stable polymer layer on the surface of a broad range of materials. The residual catechol groups on a pD layer can facilitate coupling reactions with amine and thiol groups in target molecules by Michael-type addition reactions or Schiff-

Received: April 14, 2015
Accepted: June 15, 2015
Published: June 15, 2015





DOI: 10.1021/acsami.5b03249
ACS Appl. Mater. Interfaces 2015, 7, 14415−14422

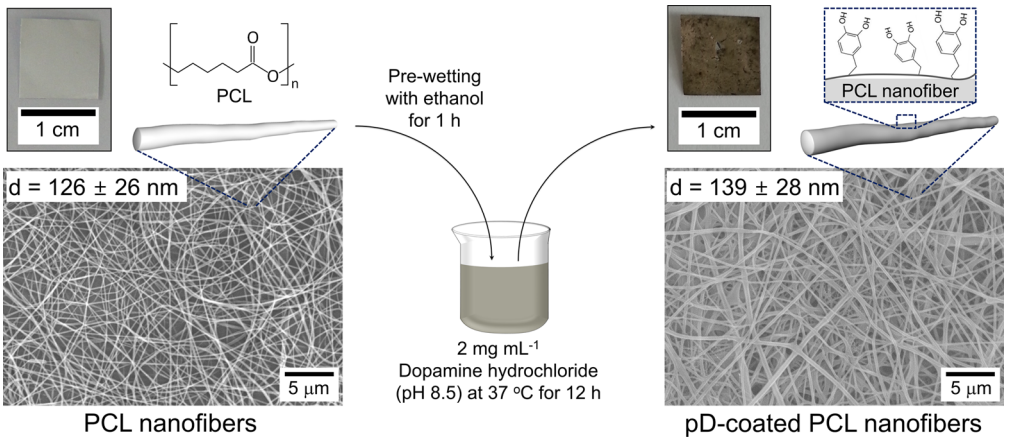


**Figure 1.** Schematic illustration of the pD coating of electrospun PCL nanofibers.

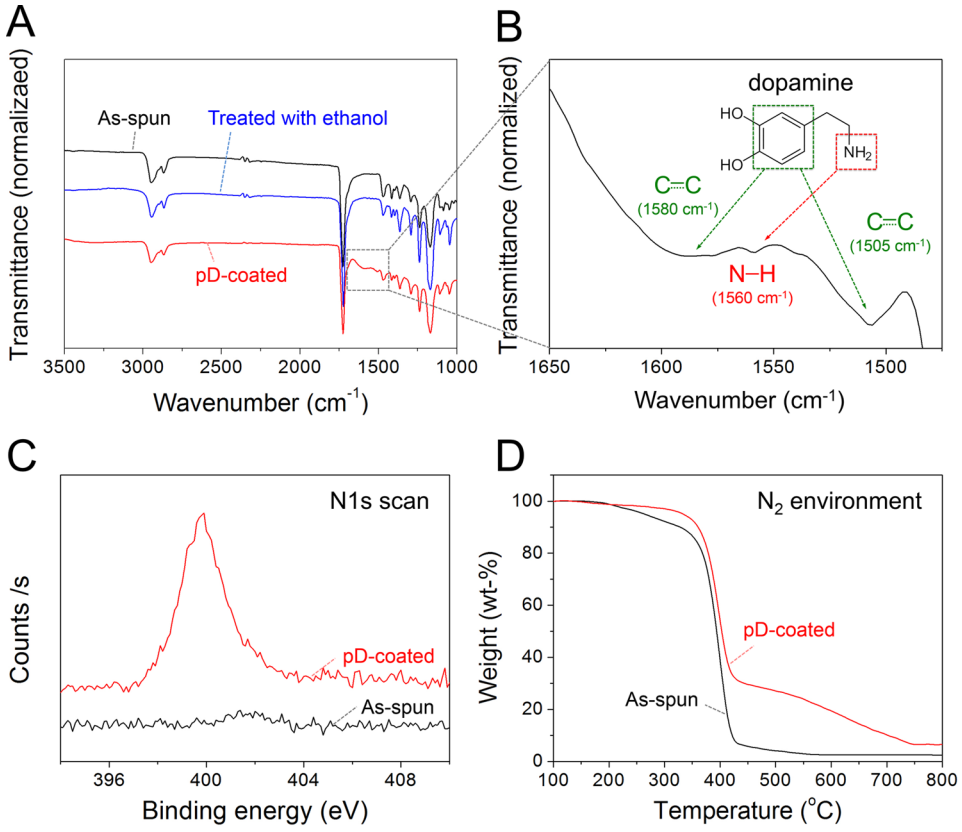


**Figure 2.** (A) ATR-IR spectra of PCL nanofibers as spun (black), after wetting with ethanol for 1 h (blue), and after pD coating for 12 h (red). (B) Enlarged ATR-IR spectrum. (C) N 1s XP spectra of PCL nanofibers as spun (black) and after pD coating for 12 h (red). (D) TGA thermograms of PCL nanofibers as spun (black) and after pD coating for 12 h (red) in nitrogen gas.

base formations. Another interesting feature of pD coatings is that the catechol moiety has a moderate reduction capability with a redox potential of 530 mV vs normal hydrogen electrode (NHE) at pH 7.[21−24] This reduction power is enough to induce the chemical reduction of metal ions, including gold, silver, and iron ions. The one-pot synthesis with dopamines and metal ions can produce a metal−pD hybrid layer on various substrates through the oxidative polymerization of dopamines and simultaneous reduction of metal ions.

In this work we utilized the pD chemistry to synthesize and immobilize gold nanoparticles (AuNPs) on electrospun poly(ε-caprolactone) (PCL) nanofibers for recyclable catalysis. The surface functionalization of electrospun PCL nanofibers was performed through the oxidative polymerization of dopamines on the electrospun PCL nanofibers.[22−24] The pD coatings enable in situ on-surface synthesis of AuNPs on the electrospun nanofibers, forming metal−polymer hybrid nanomaterials, in an aqueous solution at room temperature. The structural stability, thermal properties, and repeated catalytic performances of the AuNP−pD hybrid PCL nanofibers were investigated to demonstrate the feasibility of pD chemistry for on-surface synthesis of catalytic nanocrystals for a highly active, recyclable catalysis.


DOI: 10.1021/acsami.5b03249
ACS Appl. Mater. Interfaces 2015, 7, 14415−14422

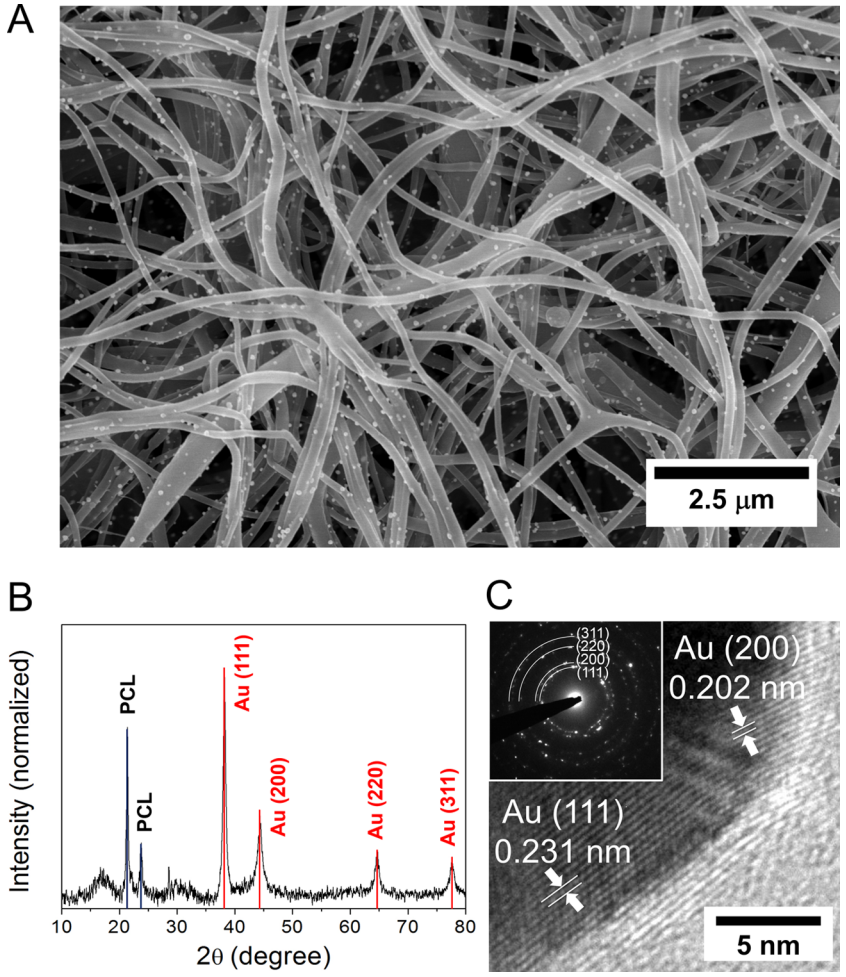


**Figure 3.** (A) SEM image of the Au–pD hybrid PCL nanofibers prepared through incubation of the pD-coated PCL nanofibers with 1 mM $HAuCl_4$ at room temperature for 24 h. (B) XRD diagram and (C) HRTEM image of the Au–pD hybrid PCL nanofibers (inset: electron diffraction pattern).

## 2. RESULTS AND DISCUSSION

The morphologies of the electrospun PCL nanofibers prepared under different experimental conditions, including the polymer concentration (8–30 wt %) and electrospinning distance, were examined to obtain a highly porous nanofibrous substrate by scanning electron microscopy (SEM) (Supporting Information, Figure S1A). Bead-like structures were dominantly formed at concentrations of the PCL solution of 8 and 10.5 wt %, while fibrous structures were generated above 14 wt %. The thickness of the nanofibers increased with the increased concentration of the polymer solution. The average diameters of the nanofibers were 73 ± 20, 98 ± 25, and 214 ± 129 nm at 14, 20, and 25 wt %, respectively. The increased thickness of the nanofibers seems to be caused by the increased viscosity of the polymer solution (Supporting Information Figure S1B). The polymer solutions were Newtonian viscous fluids as shown in the linear relationship between the shear rate and the shear stress. The calculated viscosities of the polymer solutions were 28.2, 84.1, 142.1, and 319.2 mPa s at 8, 14, 20, and 25 wt %, respectively. Silicone oil AP 100 (Aldrich 10838) was used as an internal control because of its well-known viscosity (about 100 mPa s at 25 °C). The measured viscosity of silicone oil in our experiment was 110.5 mPa s. To examine the effects of an electrospinning distance on the morphology of the nanofibers, two different electrospinning distances ($L_e$), 12.5 and 25 cm, were compared. When the PCL nanofiber flied a longer distance, the thickness of the PCL nanofibers was remarkably decreased (Supporting Information Figure S1A). Bead-free nanofibers with an average diameter of 128 ± 34 nm were generated when 2 wt % sodium dodecyl sulfate (SDS) was added to the polymer solution (25 wt %) (Supporting Information Figure S1C). The addition of SDS increased not only the viscosity of the polymer solution from 319.2 to 419.7 mPa s, but also the conductivity of the pendant droplet from 42.6 to 827.4 mS $cm^{-1}$, facilitating the elongation of the electrospinning jet and thus suppressing the formation of the beads.

The pD coatings were performed using the prepared electrospun PCL nanofibers at a PCL concentration of 25 wt % with 2 wt % SDS to functionalize their surface for chemical modification. Schematic illustration of the pD coatings onto PCL nanofibers is shown in Figure 1. pD-coated nanofibers were formed by dipping the electrospun PCL nanofibers into a dopamine solution (2 mg $mL^{-1}$, pH 8.5). The nanofibers were prewetted with ethanol for 1 h to increase their water wettability. The nanofibers were then incubated in a dopamine solution with orbital shaking at 200 rpm for 12 h. The color of the PCL nanofibers changed from white to reddish brown as the PCL nanofibers were coated with pD. The pD coating slightly increased the diameter of the electrospun nanofibers from 126 ± 26 to 139 ± 28 nm. The results indicate that the pD layer was successfully deposited onto the PCL nanofibers.


DOI: 10.1021/acsami.5b03249
ACS Appl. Mater. Interfaces 2015, 7, 14415–14422

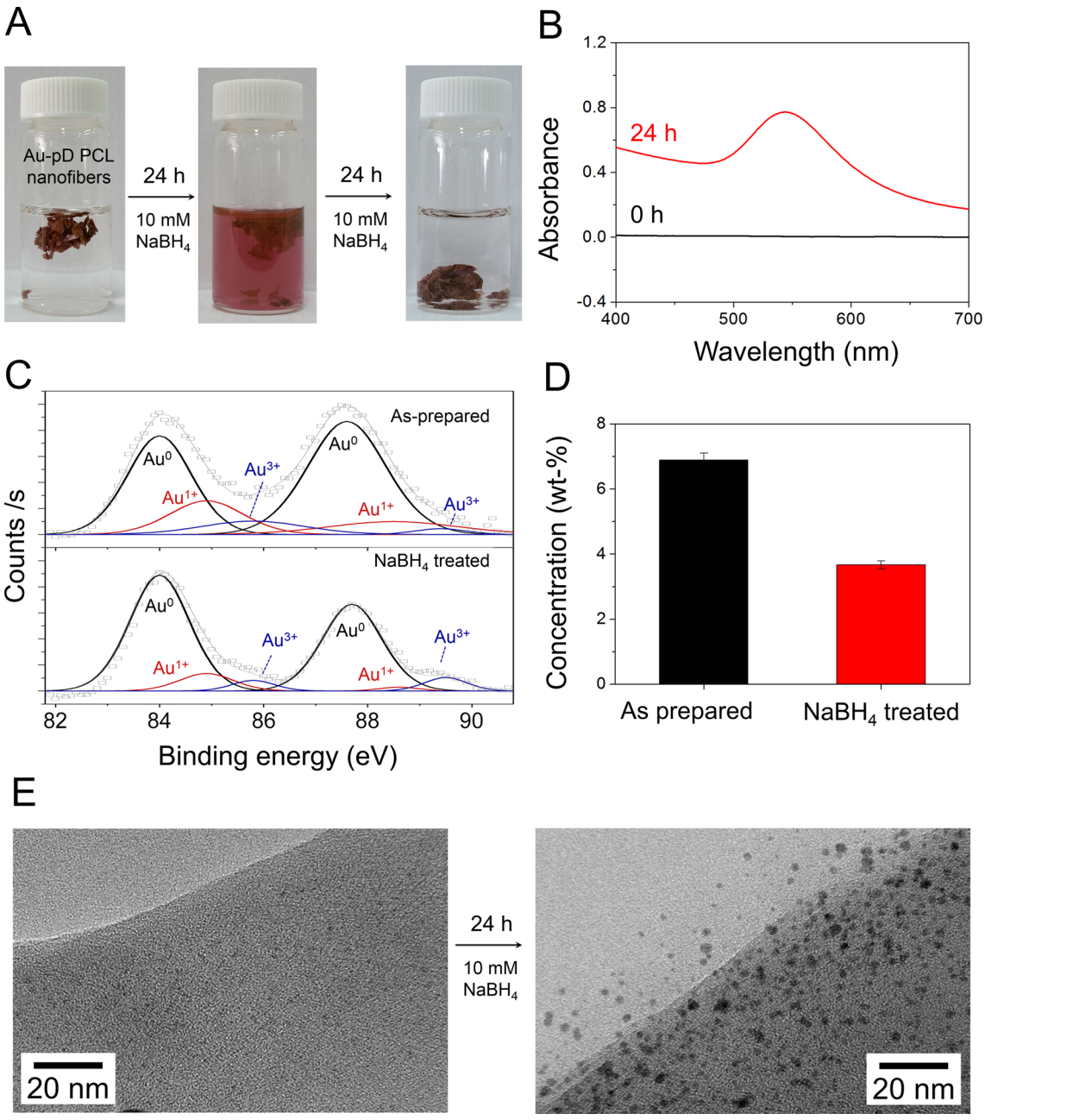


**Figure 4.** (A) Photographic images of the Au–pD hybrid nanofibers incubated in 10 mM $NaBH_4$ at 37 °C. (B) UV–vis light absorption spectra of the $NaBH_4$ solutions immersed with the Au–pD hybrid nanofibers. (C) XP spectra of the Au–pD hybrid nanofibers as prepared (top) and after $NaBH_4$ treatment (bottom). (D) Weight percentages of AuNPs in the Au–pD hybrid nanofibers as prepared (left) and after $NaBH_4$ treatment (right). (E) TEM image of Au–pD hybrid PCL nanofibers before (left) and after (right) $NaBH_4$ treatment.

Attenuated total reflection infrared spectroscopy (ATR-IR) was used to confirm the pD coating of the electrospun PCL nanofibers (Figure 2A). The peaks at 1580 and 1505 $cm^{-1}$ are assigned to the $sp^2$ hybridized C–C bond from the aromatic ring of dopamine. In addition, the peak at 1560 $cm^{-1}$ might originate from the primary amine group of dopamine (Figure 2B). On the other hand, the pristine PCL nanofibers have no specific peaks within that range. X-ray photoelectron (XP) spectroscopy analysis also showed that the pD coating generated the nitrogen element, which seem to be derived from the amine group of dopamine (Figure 2C). Thermogravimetric analysis (TGA) provides quantitative information on the pD layer (Figure 2D). Residue difference between the as-spun (uncoated) and pD-coated PCL nanofibers in a nitrogen environment at 800 °C was 4.05 wt % associated with the carbonization of the pD layer. It was reported that the carbonization yield of pure pD was around 60% in nitrogen gas at 800 °C.[25] Therefore, the result indicates that about 6.6 wt % of pD was deposited onto the PCL nanofibers through the polydopamine coating process.

The catechol groups in the pD layer on the PCL nanofibers can drive the reduction of metal ions because they have a reduction capability with a redox potential of about 530 mV versus NHE at a neutral pH.[26] Our previous works also demonstrated that Ag ions can be spontaneously reduced to metallic Ag nanoparticles on the surface of pD-coated poly(vinyl alcohol) nanofibers and poly(methyl methacrylate) microparticles.[22−24] In this work, the spontaneous reduction of


DOI: 10.1021/acsami.5b03249
ACS Appl. Mater. Interfaces 2015, 7, 14415−14422

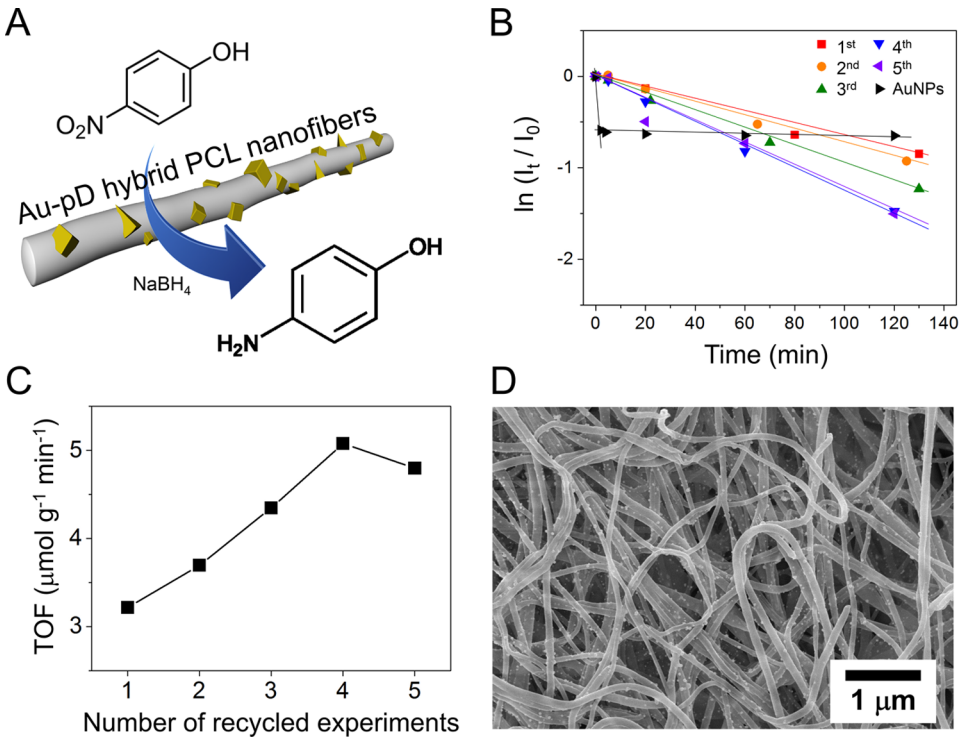


**Figure 5.** (A) Schematic illustration of the reduction of 4-NP to 4-AP by $NaBH_4$ in the presence of the Au–pD hybrid PCL nanofibers. (B) Conversion kinetics of 4-AP by the Au–pD hybrid PCL nanofibers and AuNP solution as a control experiment. The solid lines represent a linear fit to the experimental data, and the slope of the curves indicates the reaction rate constant. (C) Turnover frequencies of the number of recycled experiments for the reduction of 4-NP using the Au–pD hybrid PCL nanofibers. (D) SEM image of the A–pD hybrid PCL nanofibers after 5 cycles of catalysis.

$Au^{3+}$ ions was carried out on the surface of the pD-coated PCL nanofibers at an ambient temperature. The pD coatings made the PCL surface highly wettable, enough to perform simple dip-coating of metal ion precursors in aqueous solutions without any pretreatment. Simple immersion and the following 24-h incubation of the pD-coated PCL nanofibers in a $HAuCl_4$ solution at room temperature generated metallic AuNPs on the surface of the nanofibers (Figure 3A). Energy dispersive X-ray spectroscopy (EDX) analysis also supported the presence of Au elements in the nanofiber mats (Supporting Information Figure S2). The formation of AuNPs on the pD-coated surface was kinetically slow at an ambient temperature as only a much smaller number of AuNPs were observed at 3 and 12 h of incubation under the same conditions (Supporting Information Figure S3). Particularly, at 3 h of incubation, only a very small number of tiny AuNPs were observed on the nanofibers as indicated in Supporting Information Figure S3A. Figure 3B shows X-ray diffraction (XRD) pattern of the pD-coated PCL nanofibers incubated with the Au precursor solution at room temperature for 24 h. Four peaks observed at 38.2°, 44.4°, 64.7°, and 77.6° are well-matched with the (111), (200), (220), and (311) planes of the face-centered cubic (FCC) metallic Au, respectively (JCPDS 04-0784). High resolution transmission electron microscopic (HRTEM) analysis showed that the *d*-spacings were 0.231 and 0.202 nm, which correspond to the gold (111) and (200) planes, respectively (Figure 3C). The selected-area electron diffraction (SAED) pattern obtained from the Au–PCL hybrid nanofibers shows diffraction rings attributed to (111), (200), (220), and (311) planes of the FCC crystalline gold structure (Figure 3C, inset).

When the Au–pD hybrid PCL nanofibers were immersed in a strong reduction medium (10 mM sodium borohydride, $NaBH_4$) for 12 h at 37 °C, the color of the solution became red (Figure 4A). The UV–vis absorption spectrum showed a characteristic surface plasmon peak of AuNPs at 536.5 nm (Figure 4B). TEM analysis confirmed the formation of AuNPs dissociated from the nanofibers (Supporting Information Figure S4). XP spectroscopy revealed that the untreated Au–PCL hybrid nanostructures have 72.5% of $Au^0$, 18.4% of $Au^{1+}$, and 9.1% of $Au^{3+}$. The $NaBH_4$ treatment resulted in the increased portion of metallic $Au^0$ (85%) with the decreased percentages of $Au^{1+}$ (7.8%) and $Au^{3+}$ (7.2%) (Figure 4C). These results showed that Au ion–catechol complexes were reduced by $NaBH_4$ and eliminated from PCL nanofibers. The total loss of AuNPs as a result of $NaBH_4$ treatment was determined using inductively coupled plasma-mass spectroscopy (ICP-MS) (Figure 4D). The weight percentage of gold in the nanofibers decreased from 6.8 to 3.6 wt % as a result of the $NaBH_4$ treatment. HRTEM images that Au ion–catechol complexes and metallic AuNPs found on the surface of the Au–pD hybrid PCL nanofibers before and after the treatment with $NaBH_4$, respectively (Figure 4E). When the Au–pD hybrid PCL nanofibers were treated with fresh $NaBH_4$, no further reduction reaction of Au ions and dissociation of AuNPs were observed, indicating that AuNPs were stabilized on the surface of pD-coated PCL nanofibers.

For the evalution of the catalytic activities of the Au–pD hybrid PCL nanofibers, the reduction of 4-nitrophenol (4-NP) to 4-aminophenol (4-AP) was monitored using UV–vis light absorption spectroscopy (Figure 5A, Supporting Information Figures S5 and S6).[27−29] In a fresh $NaBH_4$ medium, the pale yellow color of the 4-NP solution turned to yellowish green rapidly, and the absorption peak of 4-NP ($\lambda_{max}$ = 320 nm) was red-shifted due to the formation of 4-nitrophenolate ions ($\lambda_{max}$


DOI: 10.1021/acsami.5b03249
ACS Appl. Mater. Interfaces 2015, 7, 14415−14422

= 400 nm). It is well-known that AuNPs can mediate the reduction of 4-nitrophenolate ions to 4-AP, which has a maximum absorption peak at 297 nm (Supporting Information Figure S7). In our work, citrate-stabilized AuNPs with an average diameter of 48.2 ± 6.9 nm were used as a control (Supporting Information Figure S8A).

The reaction rate constant, $k$, was calculated from the following equation: $\ln(I_t) = -kt + \ln(I_0)$, where $I_t$ is the absorbance at 400 nm at time $t$, and $I_0$ is the initial absorbance at 400 nm. The citrate-stabilized AuNP suspension exhibited very fast reaction kinetics ($k = 9.7 \times 10^{-2}$ min$^{-1}$) for the first 4 min of reaction. Turnover frequency (TOF), which is defined as the total number of 4-NP molecules that the catalyst with a unit weight reduces per unit time, was 778.4 $\mu$mol g$^{-1}$ min$^{-1}$, as calculated using a calibration curve of 4-NP (Supporting Information Figure S9). These results directly reflect the reduction of 4-nitrophenolate ions to 4-AP because it is hard to be adsorbed on the AuNPs and the pD−PCL nanofiber. It has been reported that 4-nitrophenol has weak interaction with the surface of AuNPs, compared to molecules that contain sulfur or large conjugated $\pi$-orbitals.[30−32] In addition, the adsorption to the pD−PCL nanofiber is not likely to occur, because both of the 4-nitrophenolate ions and the dopamine molecule have negative charges on the basis of our ab initio calculations (Supporting Information Figure S10).

However, the rate constant was rapidly decreased to 4.0 × 10$^{-4}$ min$^{-1}$ in the following stage of 4-NP reduction (Figure 5B). This rapid reduction in the catalytic activity was caused by structural instability of the citrate-stabilized AuNPs. TEM analysis showed that the AuNPs formed large aggregates and precipitates after just a few minutes of catalysis due to the reaction between highly active reducing agent and residual Au ions (Supporting Information Figure S8B and Figure 4C). On the other hand, the catalytic activity of the Au−pD hybrid PCL nanofibers were very stable and even gradually increased from 6.9 × 10$^{-3}$ to 1.2 × 10$^{-2}$ min$^{-1}$ for 5 cycles of catalysis (Figure 5B), which correspond to TOFs of 3.2−5.1 $\mu$mol g$^{-1}$ min$^{-1}$ (Figure 5C). These values are about 3 times higher than the TOF of calcium alginate gel beads incorporating AuNPs, which exhibited the highest TOF of AuNPs for the same reaction.[27] The reason why the catalytic activitiy of the Au−pD hybrid PCL nanofibers increased for the first 4 cycles is not clear. It was suspected that the partially reduced species of gold ions might be further reduced to catalytically active metallic AuNPs; however, their residual percentages were only about 15% (7.8% for $Au^{1+}$ and 7.2% for $Au^{3+}$) after the $NaBH_4$ treatment (Figure 4C), which cannot explain the 1.6 times higher TOF in the final cycle of catalysis. Therefore, we suspected that the distribution of AuNPs in the pD layer might be altered when the catalytic experiments were repeated. However, SEM and TEM images of the Au−pD hybrid nanostructures did not show any significant changes in the distribution of AuNPs (Figure 5D and Supporting Information Figure S11). The increased catalytic activity of the Au−pD hybrid nanostructures could be ascribed to very subtle structural changes (e.g., the change of crystalline facets exposed to the surface), which cannot be apparently observed by conventional electron microscopies. High resolution TEM analysis is underway to determine the precise causes of the increased activity over the repeated reactions. Despite the limitation of the current study in explaining the underlying mechanism on the increased catalytic activities, this work clearly demonstrates that the structural integrity and high catalytic activity of the Au−pD hybrid PCL nanofibers can be maintained during the repeated recycles. The maximum catalytic conversion efficiencies using Au−pD hybrid PCL nanofibers and AuNPs were 74% and 55%, respectively (Supporting Information Figure S12).

## 3. CONCLUSION

This report described a very simple method to prepare metal−polymer hybrid nanostructures via mussel-inspired polydopamine chemistry, which was utilized for the reduction and deposition of metal precursor ions on the surface of electronspun polymer nanofibers. The polydopamine played as a very stable adhesive layer that can maintain the large surface area of nanometer-sized colloidal catalysts for the high catalytic activity per mass of catalysts. The formation of a catalytically stable polydopamine interface enabled the repeated, long-term uses of nanocatalysts. In addition, the recovery and separation of catalysts in their neat form from reactants and products was possible. Therefore, we believe that the polydopamine chemistry can provide a very straightforward, simple approach to stable immobilization of nanosized catalysts for various practical applications.

## 4. EXPERIMENTAL SECTION

**Electrospinning of PCL Nanofibers.** PCL ($M_W$ = 80 kDa, Sigma-Aldrich, St. Louis, MO) was dissolved in a 9:1 mixture of formic acid and acetic acid at concentrations of 8, 10.5, 14, 17, 20, 23, 25, and 30 wt %. Two different electrospinning distances, 12.5 and 25 cm, between a needle and a collection aluminum plate were used. The electrospinning voltage was fixed to 18 kV using a voltage generator (CPS-40 K03VIT, Chungpa EMT, Seoul, Republic of Korea). The polymer solution was injected at 0.6 mL h$^{-1}$ using a syringe pump (model 781100, KD Scientific Inc., Holliston, MA) with a stainless steel needle (22 gauge).

**Synthesis of Citrate-Stabilized AuNPs.** A 50 mL aqueous solution of 0.25 mM $HAuCl_4$ (Sigma-Aldrich) was heated to boiling, and 0.4 mL of 1 wt % trisodium citrate was added under continueous magnetic stirring. After 30 min boiling and stirring, the resulting AuNP suspension was dialyzed against an excess amount of deionized water to remove residual precursor and citrate ions.

**On-Surface Synthesis of AuNPs on Nanofibers.** Dopamine hydrochloride (Sigma-Aldrich) was dissolved in deionized water at a concentration of 2 mg mL$^{-1}$. The electrospun PCL nanofibers were immersed in ethanol for 1 h and then transferred to the dopamine solution. To the dopamine solution (100 mL) was added 0.1 M NaOH (2 mL, Sigma-Aldrich) to adjust pH to 8.5. The electrospun PCL nanofibers were incubated in the dopamine solution with orbital shaking at 200 rpm for 12 h. The prepared pD-coated PCL nanofibers were then incubated in 1 mM $HAuCl_4$ in deionized water to generate AuNP−pD hybrid PCL nanofibers. All of the synthetic procedures were carried out at an ambient temperature.

**Measurements of Catalytic Activity.** The catalytic activity of the Au−PCL hybrid nanofibers as a substrate was determined using 4-NP (Sigma-Aldrich). Briefly, 0.1 mM of 4-NP in deionized water (3 mL) was mixed with 300 mM of $NaBH_4$ (100 $\mu$L, Sigma-Aldrich). Then, a 10 mg portion of Au-PCL hybrid nanostructures was immersed in the prepared mixture. For a control experiment, 1.5 mL of 0.2 mM 4-NP was mixed with 100 $\mu$L of 300 mM $NaBH_4$, and then 1.5 mL of the prepared AuNP suspension was added. 4-AP was purchased from Sigma-Aldrich for the standard absorption spectra.

**Characterization.** The PCL solution conductivities were measured using an ORION Star A212 conductivity meter (013005MD conductivity cell, Thermo Scientific). The nanofiber samples were analyzed using ATR-IR (Bruker Optiks Hyperion 3000, Germany) and multipurpose XP spectroscopy (Sigma Probe, Thermo VG Scientific). The morphology of the prepared nanofibers was examined using SEM (Hitachi S-4800, Tokyo, Japan) at an acceleration voltage of 10 kV after platinum coating of about 3 nm thick. The diameter of the


DOI: 10.1021/acsami.5b03249
ACS Appl. Mater. Interfaces 2015, 7, 14415−14422

nanofibers was determined from at least 100 sample spots in SEM images using the ImageJ software (U.S. National Institute of Health). The nanoparticles were observed using TEM (JEOL JEM-3011 HR, Japan) at an acceleration voltage of 300 kV. TGA (TG 209 F3, NETZSCH-Gerätebau GmbH, Selb/Bavaria, Germany) was performed at a heating rate of 10 °C $min^{-1}$ in air. The reduction of 4-NP was monitored by the change of absorbance at 400 nm using UV−vis light absorption spectroscopy (UV-1800, Shimadzu Corp., Kyoto, Japan).

**Ab Initio Calculations.** The computational method was used for the molecular geometry optimizations and the calculation of the atomic charges of a 4-nitrophenolate ion and a dopamine molecule, where a quinone was calculated because of the strong basic condition of the solution (pH 9.9). All calculations were performed using the Gaussian03 software package with the B3LYP hybrid functional and the 6-31+G(d) basis set.[33] All geometries were fully optimized, and the Mulliken population analysis was performed for the calculation of the atomic charges.

## ■ ASSOCIATED CONTENT

### Supporting Information

Additional figures, including characterization details. The Supporting Information is available free of charge on the ACS Publications website at DOI: 10.1021/acsami.5b03249.

## ■ AUTHOR INFORMATION


### Corresponding Author

*E-mail: yoonsung@kaist.ac.kr.

### Author Contributions

I.K. and H.Y.S. contributed equally to this work.


### Notes

The authors declare no competing financial interest.

## ■ ACKNOWLEDGMENTS

This work was supported by the Korea CCS R&D Center (KCRC), Basic Science Research, and Nano·Material Technology Development Programs through the National Research Foundation of Korea (NRF) funded by the Ministry of Science, ICT & Future Planning (NRF-2014M1A8A1049303, NRF-2013R1A1A1009626, and NRF-2012M3A7B4049802).

## ■ REFERENCES


(1) El-Sayed, M. A. Some Interesting Properties of Metals Confined in Time and Nanometer Space of Different Shapes. *Acc. Chem. Res.* **2001**, *34* (4), 257−264.

(2) Pozzo, R. L.; Baltanas, M. A.; Cassano, A. E. Supported Titanium Oxide as Photocatalyst in Water Decontamination: State of the Art. *Catal. Today* **1997**, *39* (3), 219−231.

(3) Magrez, A.; Horvath, L.; Smajda, R.; Salicio, V.; Pasquier, N.; Forro, L.; Schwaller, B. Cellular Toxicity of $TiO_2$-Based Nanofilaments. *ACS Nano* **2009**, *3* (8), 2274−2280.

(4) Nam, Y. S.; Magyar, A. P.; Lee, D.; Kim, J. W.; Yun, D. S.; Park, H.; Pollom, T. S.; Weitz, D. A.; Belcher, A. M. Biologically Templated Photocatalytic Nanostructures for Sustained Light-Driven Water Oxidation. *Nat. Nanotechnol.* **2010**, *5* (5), 340−344.

(5) Lee, J. A.; Nam, Y. S.; Rutledge, G. C.; Hammond, P. T. Enhanced Photocatalytic Activity Using Layer-by-Layer Electrospun Constructs for Water Remediation. *Adv. Funct Mater.* **2010**, *20* (15), 2424−2429.

(6) Jeong, C. K.; Kim, I.; Park, K. I.; Oh, M. H.; Paik, H.; Hwang, G. T.; No, K.; Nam, Y. S.; Lee, K. J. Virus-Directed Design of a Flexible $BaTiO_3$ Nanogenerator. *ACS Nano* **2013**, *7* (12), 11016−11025.

(7) Dotzauer, D. M.; Dai, J. H.; Sun, L.; Bruening, M. L. Catalytic Membranes Prepared Using Layer-by-Layer Adsorption of Polyelectrolyte/Metal Nanoparticle Films in Porous Supports. *Nano Lett.* **2006**, *6* (10), 2268−2272.

(8) White, R. J.; Luque, R.; Budarin, V. L.; Clark, J. H.; Macquarrie, D. J. Supported Metal Nanoparticles on Porous Materials. Methods and Applications. *Chem. Soc. Rev.* **2009**, *38* (2), 481−494.

(9) Zhang, Y.; Crittenden, J. C.; Hand, D. W.; Perram, D. L. Fixed-Bed Photocatalysts for Solar Decontamination of Water. *Environ. Sci. Technol.* **1994**, *28* (3), 435−442.

(10) Xu, Y. M.; Langford, C. H. Enhanced Photoactivity of a Titanium(IV) Oxide-Supported on ZSM5 and Zeolite A at Low-Coverage. *J. Phys. Chem.* **1995**, *99* (29), 11501−11507.

(11) Bellobono, I. R.; Bonardi, M.; Castellano, L.; Selli, E.; Righetto, L. Degradation of Some Chloro-Aliphatic Water Contaminants by Photocatalytic Membranes Immobilizing Titanium-Dioxide. *J. Photochem. Photobiol., A* **1992**, *67* (1), 109−115.

(12) Nair, M.; Luo, Z. H.; Heller, A. Rates of Photocatalytic Oxidation of Crude-Oil on Salt-Water on Buoyant, Cenosphere-Attached Titanium-Dioxide. *Ind. Eng. Chem. Res.* **1993**, *32* (10), 2318−2323.

(13) Nam, Y. S.; Park, T. G. Porous Biodegradable Polymeric Scaffolds Prepared by Thermally Induced Phase Separation. *J. Biomed. Mater. Res.* **1999**, *47* (1), 8−17.

(14) Nam, Y. S.; Yoon, J. J.; Park, T. G. A Novel Fabrication Method of Macroporous Biodegradable Polymer Scaffolds Using Gas Foaming Salt as a Porogen Additive. *J. Biomed. Mater. Res.* **2000**, *53* (1), 1−7.

(15) Reneker, D. H.; Yarin, A. L. Electrospinning Jets and Polymer Nanofibers. *Polymer* **2008**, *49* (10), 2387−2425.

(16) Lim, Y.-M.; Gwon, H.-J.; Shin, J.; Jeun, J. P.; Nho, Y. C. Preparation of Porous Poly(ε-Caprolactone) Scaffolds by Gas Foaming Process and in Vitro/in Vivo Degradation Behavior Using γ-Ray Irradiation. *J. Ind. Eng. Chem.* **2008**, *14* (4), 436−441.

(17) Li, D.; Xia, Y. N. Electrospinning of Nanofibers: Reinventing the Wheel? *Adv. Mater.* **2004**, *16* (14), 1151−1170.

(18) Nam, Y. S.; Park, T. G. Biodegradable Polymeric Microcellular Foams by Modified Thermally Induced Phase Separation Method. *Biomaterials* **1999**, *20* (19), 1783−1790.

(19) Carlberg, B.; Ye, L. L.; Liu, J. Surface-Confined Synthesis of Silver Nanoparticle Composite Coating on Electrospun Polyimide Nanofibers. *Small* **2011**, *7* (21), 3057−3066.

(20) Lee, H.; Dellatore, S. M.; Miller, W. M.; Messersmith, P. B. Mussel-Inspired Surface Chemistry for Multifunctional Coatings. *Science* **2007**, *318* (5849), 426−430.

(21) Lee, Y.; Park, T. G. Facile Fabrication of Branched Gold Nanoparticles by Reductive Hydroxyphenol Derivatives. *Langmuir* **2011**, *27* (6), 2965−2971.

(22) Son, H. Y.; Lee, D. J.; Lee, J. B.; Park, C. H.; Seo, M.; Jang, J.; Kim, S. J.; Yoon, M. S.; Nam, Y. S. In Situ Functionalization of Highly Porous Polymer Microspheres with Silver Nanoparticles via Bio-Inspired Chemistry. *RSC Adv.* **2014**, *4* (98), 55604−55609.

(23) Son, H. Y.; Ryu, J. H.; Lee, H.; Nam, Y. S. Bioinspired Templating Synthesis of Metal-Polymer Hybrid Nanostructures within 3D Electrospun Nanofibers. *ACS Appl. Mater. Interfaces* **2013**, *5* (13), 6381−6390.

(24) Son, H. Y.; Ryu, J. H.; Lee, H.; Nam, Y. S. Silver-Polydopamine Hybrid Coatings of Electrospun Poly(vinyl alcohol) Nanofibers. *Macromol. Mater. Eng.* **2013**, *298* (5), 547−554.

(25) Liu, R.; Mahurin, S. M.; Li, C.; Unocic, R. R.; Idrobo, J. C.; Gao, H. J.; Pennycook, S. J.; Dai, S. Dopamine as a Carbon Source: The Controlled Synthesis of Hollow Carbon Spheres and Yolk-Structured Carbon Nanocomposites. *Angew. Chem., Int. Ed.* **2011**, *50* (30), 6799−6802.

(26) Steenken, S.; Neta, P. One-Electron Redox Potentials of Phenols. Hydroxy- and Aminophenols and Related Compounds of Biological Interest. *J. Phys. Chem* **1982**, *86* (18), 3661−3667.

(27) Saha, S.; Pal, A.; Pande, S.; Sarkar, S.; Panigrahi, S.; Pal, T. Alginate Gel-Mediated Photochemical Growth of Mono- and Bimetallic Gold and Silver Nanoclusters and Their Application to Surface-Enhanced Raman Scattering. *J. Phys. Chem. C* **2009**, *113* (18), 7553−7560.

(28) Saha, S.; Pal, A.; Kundu, S.; Basu, S.; Pal, T. Photochemical Green Synthesis of Calcium-Alginate-Stabilized Ag and Au Nano-




DOI: 10.1021/acsami.5b03249
*ACS Appl. Mater. Interfaces* 2015, 7, 14415−14422

particles and Their Catalytic Application to 4-Nitrophenol Reduction. *Langmuir* **2010**, *26* (4), 2885−2893.
(29) Lin, C.; Tao, K.; Hua, D. Y.; Ma, Z.; Zhou, S. H. Size Effect of Gold Nanoparticles in Catalytic Reduction of p-Nitrophenol with $NaBH_4$. *Molecules* **2013**, *18* (10), 12609−12620.
(30) Pozun, Z. D.; Rodenbusch, S. E.; Keller, E.; Tran, K.; Tang, W.; Stevenson, K. J.; Henkelman, G. A Systematic Investigation of -Nitrophenol Reduction by Bimetallic Dendrimer Encapsulated Nanoparticles. *J. Phys. Chem. C* **2013**, *117* (15), 7598−7604.
(31) Hakkinen, H. The Gold-Sulfur Interface at the Nanoscale. *Nat. Chem.* **2012**, *4* (6), 443−455.
(32) Wheeler, W. D.; Parkinson, B. A.; Dahnovsky, Y. The Adsorption Energy and Diffusion of a Pentacene Molecule on a Gold Surface. *J. Chem. Phys.* **2011**, *135* (2), 024702.
(33) *Gaussian 03, Revision C. 02*; Gaussian, Inc.: Wallingford, CT, 2004.


DOI: 10.1021/acsami.5b03249
*ACS Appl. Mater. Interfaces* 2015, 7, 14415−14422